Fire Technology, 55, 1451-1475, (2019) :

Thermal path reconstruction for reinforced concrete under fire

Paola Meloni · Fausto Mistretta · Flavio Stochino · Gianfranco Carcangiu

Received: date / Accepted: date

Abstract In post-fire investigation, the damage of fire-exposed concrete is usually related to the temperature time-history.

This paper presents the results of an experimental investigation on reinforced concrete, cement pastes and mortars exposed to fire, aimed at identifying the benchmarks necessary to reconstruct the thermal path 15 dry core samples were obtained from a real fire damaged structure and compared to other reference dry cores collected in not damaged zones of the same structure. In addition, 16 irregular spalling samples were collected and investigated. In order to assess changes in mineralogical composition and microstructure modifications due to temperature, 20 cubic cement pastes samples and 20 prismatic mortars specimens were realized and exposed to temperature ranging from 200°C up to 800°C with a gradient of 10°C/min and keeping the maximum temperature for 1h.

Optical and Scanning Electron Microscopy, X-Ray Diffraction, Thermoanalysis and MIP porosimetry along with Helium picnometry allowed to investigate the damage degree and the mineralogical changes of the concrete and other cement based materials. Calibrated Colorimetry could determine fire temperature in the different parts of the samples due to colour changes in the mineralogical phases and in the microstructure of cement materials.

P. Meloni
Department of Mechanical, Chemical and Material Engineering, University of Cagliari. ITALY.
E-mail: paola.meloni@unica.it

F. Mistretta
Department of Civil, Enviromental Engineering and Architecture, University of Cagliari. ITALY.
E-mail: fmistret@unica.it

F. Stochino
Department of Civil, Enviromental Engineering and Architecture, University of Cagliari. ITALY.
Corresponding author
E-mail: fstochino@unica.it

G. Carcangiu
National Research Council, UOS of Cagliari. ITALY
E-mail: g.carcangiu@isac.cnr.it

The absence or presence of some specific minerals (like Portlandite), the colorimetric variations and other microstructural features are markers capable of assessing the temperature reached with high accuracy. The approach and the data showcased in this work can be useful for post-fire investigations, for theoretical and numerical models tuning and to optimize the structural retrofitting.

Keywords Fire damages · Cement · Reinforced Concrete · Colorimetry · Porosimetry · Microscopy · Mineralogical Composition

1 Introduction

If exposed to fire, reinforced concrete (RC) and cement-based materials can be damaged depending on the thermal path of the event, which can be influenced by many variables. The extent of the concrete damage due to fire-exposure depends on the characteristics of the materials and their spatial structuring; the nature of the aggregates, the composition of the cement, their mix design, the arrangement of the reinforcements and their stress state [1] - [2] - [3]- [4] - [5]. In addition, the specific fire scenario strongly [6] - [7] modifies the damage. An important role is also played by the thermal expansion coefficients of the reinforced concrete components [5]. The fire induced damages range from a slight microfracture, up to the total separation of the aggregates from the cement paste, the spalling of the concrete, the formation of millimeter lumen fractures, until its complete pulverization [5] - [8] - [9] .

Many methods can be applied to evaluate the characteristics of post-fire damage and the temperature time history [10]: the residual resistance of some structural elements [11], the ultrasound propagation velocity [12], the compressive strength and the tensile stress resistance of cylindrical specimens resulting from the dry coring of the involved structures [13] can provide important information on material deterioration. The most common outcomes of high temperature exposure of reinforced concrete are deformation, fracturing, disintegration and explosive spalling. Indeed, fire can be often followed or anticipated by an explosion and, in this case, materials and structures are pushed to their limits [14] - [15].

A reliable reconstruction of the temperature distribution can be obtained integrating the data resulting from the above mentioned techniques with those produced by other systems which investigate the microstructural and mineralogical changes. Optical Microscopy and Scanning Electron Microscopy [8] - [9] - [16], are among the most effective techniques to assess the damages suffered by the microstructures of the reinforced concrete (debonding, micro-cracking, secondary porosity, delamination, etc.).

Changes in mineralogical composition of concrete [17] - [18], with the occurrence or disappearance of mineralogical phases that can be used as geo-thermometers, can be investigated using X-ray diffraction (XRD) techniques and differential thermal analysis (TG-DTA).

Also Mecrury Intrusion Porosimetry (MIP) carried out on cement based materials subjected to heat treatment, provides important indications on microstructural changes of the porous network [19].

The changes induced by heat treatment are related to the dehydration of the calcium silicates (CSH) and calcium aluminates hydrates (CAH) gels that lose

Please cite this document as: Meloni P., Mistretta F., Stochino F., Carcangiu G. Thermal Path Reconstruction for Reinforced Concrete Under Fire, Fire Technology, 55, 1451-1475, (2019)

the adsorbed, capillary and interstitial water at different temperatures and to the debonding in the transition zone. Also the dehydroxilation of Portlandite causes a significant increase of porosity. With carbonate aggregates at high temperatures ($> 750\ ^{\circ}C$) fracturation and decarbonation occur, leading to a notable increase in porosity with the formation of the relative Ca or Mg oxides. The porosity changes affect many physical properties of the concrete, such as permeability, mechanical strength and durability [20] - [21] - [22].

Moreover, the chromatic changes of the exposed concrete, see [23], are other significant parameters. For example, the colour shift related to a particular oxidation rate of the different chromophore elements, especially Fe, enables the assessment of a given range of temperature. Actually, the chromatic change related to the chemical-mineralogical nature of the concrete constituents exposed to fire, can point the achievement of certain temperatures, which can trigger a more or less intense crack pattern. The color change is not directly related to the loss of performance, but its main cause is the crack pattern responsible for the strength reduction [24]. However, the color change can be a useful indicator to identify the achievement of certain thermal conditions and corresponding damage. A set of material properties variations yields to the material degradation and to thermal conductivity alteration. Similarly to ultrasonic test, also the measurement of the porosity (from microcrack up to micropores) of concretes exposed to different temperatures, can indirectly highlight the reduction of the mechanical strength and the variation of the elastic modulus [12], [25], [26], [27], [28] [29]. Different mathematical relationships have been proposed by various authors (such as [30], [31], [32], [33]) to indicate the relationships between compressive strength, Young Modulus and porosity of concrete. Thus, the analysis of porosimetry data, related to different damaged concrete, could be obtained to evaluate the thermal conductivity and other physical properties [34], [35].

This paper presents the results of an experimental investigation on reinforced concrete, cement pastes and mortars exposed to fire, aimed at identifying the benchmarks necessary to reconstruct the thermal path.

On the evening of November 16, 2013 a fire spread through a RC industrial warehouse located in the outskirts of Cagliari (Italy). The fire lasted approximately eight hours and damaged the central part of the building. For interested readers more information can be found in [13]-[36]-[37]. In situ numerous samples of mortar cement and of concrete were taken at different depths, including pieces resulting from thermal spalling. In addition, numerous samples were obtained from core drilling of the concrete damaged building in differently degraded sectors. Also a non-degraded core has been used as a reference. These cores, with a maximum length of 60 cm, were subject to laboratory investigations [13]. The experimental investigations aimed at reconstructing the thermal path and the concrete damage often require a change of scale from concrete to cement paste. The adopted "artificial" samples were made with aggregates, additives, cement and concrete mix design very similar to those that characterize the real concrete exposed to fire scenario. In particular cement mortars were subject to sampling from cores or other specimens. To reduce the disturbance created by sampling, percussive methods have been excluded to privilege the use of microtomes and diamond saws of high precision and stability. The thermally stressed samples were incorporated in a resin in order to make the necessary cuts.

Please cite this document as: Meloni P., Mistretta F., Stochino F., Carcangiu G. Thermal Path Reconstruction for Reinforced Concrete Under Fire, Fire Technology, 55, 1451-1475, (2019)

The comparison of the fire effects and the mineralogical, physical and mechanical changes between the artificially damaged samples and the in situ ones lead to the identification of the main isothermal lines (e.g. 300°C, 500°C and 700°C). Thus, data obtained with this analysis could be used not only to improve the accuracy of numerical models of possible fire scenarios but also to optimize the demolition and reconstruction of damaged concrete structures.

2 Materials and methods

2.1 Sample preparation

In order to assess the severity of damage on a concrete structure exposed to fire and the corresponding thermal path, 15 cylindrical samples (diameter 6 cm and variable length), were taken in different parts of the building by means of dry coring, as well as 15 irregularly shaped samples, resulting from explosive spalling together with an undamaged sample. Moreover, 20 prismatic samples (4x4x4 cm) of cement paste and 20 prismatic samples (4x4x16 cm) mortars (CEM I 52.5 R), with water/cement ratio = 0.5, 3-years aged, and carbonatic fine sand aggregates for mortars with cement sand ratio equal to 0.33 ratio were investigated. This water to cement ratio has been adopted in order to have an effective workability of mortars made with a carbonate aggregate (2 mm to 0.063 mm size) obtained by artificial crushing of a local limestone. These aggregates have the same mineralogical nature as those present in the concrete of the considered industrial warehouse subjected to fire. The mortars were cast in standard steel formworks and matured in a saturated thermostatic cabinet (T=200.5° and UR$\geq$ 95%). From these samples, some fragments of cement paste and aggregates were taken at different depths. The fragments have been micronized by using an agate mortar in order to obtain suited powders for different investigations, see Figure 1a. Taking into account the materials microstructural complexity, 3 specimens for each sample were analyzed in order to optimize the results of the investigations and increase the accuracy.

2.2 Thermal Treatment

In a real dynamic fire scenario very complex phenomena occur involving the diffusion of energy and matter together with the chemical, morphological and structural modifications of the reinforced concrete. Many authors have investigated these effects and also those caused by a very high heating rate that produce explosive spalling, fragmentation, pulverization until the formation of vitrified crusts on concrete ([38], [39], [40], [41]).

The undamaged samples coming from the dry coring have been subjected to thermal treatment (TT) into an electric programmable oven [1]. The rate and the duration of the heating process was established on the basis of preliminary tests, depending on the real fire scenario. Test temperatures ranged from the initial 100°C up to 800°C. A heating rate of 10°C/min was adopted to reach the peak temperature for each cycle; the sample was held at that temperature for one hour.

[1] model Nabertherm LHT/0216

Please cite this document as: Meloni P., Mistretta F., Stochino F., Carcangiu G. Thermal Path Reconstruction for Reinforced Concrete Under Fire, Fire Technology, 55, 1451-1475, (2019)

(a) Specimens preparation (b) Scanning Electron Microscopy

(c) X-Rays Diffraction Analysis (d) Differential Thermal Analysis

(e) Optical Microscopy (f) Mercury Intrusion Porosimetry

Fig. 1 Laboratory test setup.

The heating rate was chosen given the information emerged from the inspections on the fired building and from the scientific literature. Indeed many authors adopted this heating rate to obtain concrete spalling and cracking: [38], [42], [43], [44].

The artificially damaged samples (TT), providing a specific calibration system, have been subjected to the same diagnostic routine performed for in situ samples.

Please cite this document as: Meloni P., Mistretta F., Stochino F., Carcangiu G. Thermal Path Reconstruction for Reinforced Concrete Under Fire, Fire Technology, 55, 1451-1475, (2019)

2.3 Optical Microscopy (OM)

The instrument used for the observation of the thin sections or fragments of cement pastes and mortars is a Carl Zeiss Axioscope 40, an optical microscope equipped with HR Axiocam, working with plain polarized transmitted light (PPTL mode), cross polarized light (CPL mode), reflection light (RL mode) and ultra violet fluorescent light (UVFL mode), see Figure 1e.

2.4 X-Rays Diffraction (XRD) Analyses

XRD spectra were acquired on powders according to the following instrumental conditions: Cukα radiation, 15 kV, 30 mA, Ni filter, 3-90 $^\circ$ 2θ scan, sampling step 0.02 $^\circ$ 2θ, acquisition rate 0.2 $^\circ$ 2θ/ min, graphite monochromator, see Figure 1c. The identification of minerals was carried out using the search Crystal Impact MATCH software which uses, for comparison, both the JCPDS Database (Joint Committee on Powder Diffraction), and the COD Database (Crystallography Open Database [45]).

2.5 Thermal gravimetric and Differential Thermal Analyses (TG-DTA)

TG-DTA have been carried out by means of a Netsch Jupiter 499 IV operating at a heating rate of 10°C/min up to a temperature of 1100°C, flushing a 80-20 mixture of nitrogen and oxygen at a 80 l/min rate. Raw data have been processed by Proteus software, see Figure 1d.

2.6 Mercury Intrusion Porosimetry (MIP)

Porosimetric measurements were performed with a Micromeritics Autopore IV 9500 Porosimeter, Hg Forced Intrusion (MIP), operating until 2200 bars, with an equilibration time equal to 10 sec. Fragments of about 2 cm^3 of cement based material were dried at 60°C for 24 hours, then placed in a Silica gel desiccator until cooling and finally weighed. The density and the volume of every sample were measured using a He Picnometer (Micromeritics AccuPycII 1340 V2.00) before and after the thermal treatments, see Figure 1f. The corresponding values were introduced in the material parameter routine of the MIP Autopore software.

2.7 Scanning Electron Microscopy (SEM) and Energy Dispersive Spectroscopy (EDS)

Thin sections have been observed with Scanning Electron Microscopy (SEM), after gold sputtering of the samples. A Zeiss Evo SEM LS15 microscopy equipped with a LaB6 crystal as electron source was used to perform Scanning Electron Microscopy and (SEM-EDS) analysis at an accelerated 15keV voltage, see Figure 1b.

Please cite this document as: Meloni P., Mistretta F., Stochino F., Carcangiu G. Thermal Path Reconstruction for Reinforced Concrete Under Fire, Fire Technology, 55, 1451-1475, (2019)

2.8 Colorimetric investigations

Colorimetric measurements have been performed by means of Konica Minolta CM 700d/600d spectrophotometer and a SAV template 3 mm in diameter. The applied colour space is CieLab 76 Illuminant D65, Observer 10°, characterized by a number of averaging equal to 6 for each measure. Some cylindrical samples of the undamaged specimen have been cut with a saw plane and polished in order to measure the colour of aggregates of the mortars and of the cement paste.

3 Results and discussion

3.1 OM and SEM investigations

Optical Microscopy (OM) and SEM investigations are indispensable tools for the reconstruction of the temperature-path of concrete exposed to fire. They allow to analyse the changes in the microstructure and its mineralogy variations [46], [47]. The information acquired through the microstructural and morphological analysis of cement based samples exposed to fire allow to assess the damage degree that influences the mechanical performance The quantification of defects can be obtained by measurement on the microcracks network [8], [9], [16], [46], [47], [48]. Specific image analysis software can be a useful tool [9]. The reference unaltered samples observed using optical microscopy (PPTL, RL, CPL and UVFL mode), show very compact aggregates of carbonatic nature (e.g. calcite and dolomite) immersed in a cement matrix unaffected by carbonation and secondary porosity. Microfractures and debonding are absent in the interfacial zone as revealed by UVFL mode observations; only a major fluorescence activity (bright green) can be observed in correspondence of the transition zone (Figure 2) due to its different fabric characterized by higher porosity and higher presence of Portlandite. SEM observations confirmed the integrity of the microstructure and revealed some mineralogical components of cement such as silicates (CSH), calcium aluminates (CAH) hydrates as well as Portlandite and needle-like crystals of ettringite, see Figure 3. Conversely, concrete after severe and very severe damages presents an important loss of performance, such as pulverization, fracturing, detachement of aggregates. Microscopy UVFL observations, also at different depths, of samples exposed to high temperatures, assess a common zoning: total decohesion between cement matrix and aggregates as well pervasive microfracturing and secondary diffuse porosity, Figure 4.

SEM observations allow to follow the evolution of microstructural modifications as a result of heat treatment at various temperatures. These changes begin to be relevant at around 300 °C and consist in a widespread microfracture system in the cement matrix, detachments in the transition zone followed by detachment, granular disintegration and pulverization as the temperature increases up to 750÷800 °C (Figure 5). The extent of the detachments in the transition zone at temperatures above 300°C are linked to the nature of the aggregates (quartzosilicate aggregates are generally more harmful than carbonate ones) and also to the thermal properties of all the constituents of the concrete [5]

RL observations allow to have a more realistic idea of the actual damage suffered by the cement matrix and the concrete exposed to the heat treatment, with

Please cite this document as: Meloni P., Mistretta F., Stochino F., Carcangiu G. Thermal Path Reconstruction for Reinforced Concrete Under Fire, Fire Technology, 55, 1451-1475, (2019)

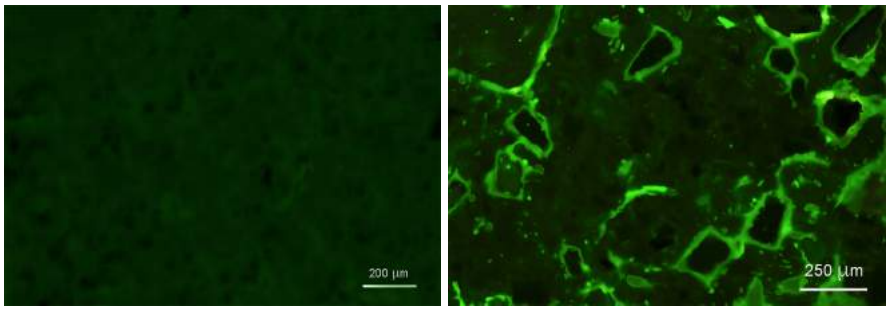

(a) (b)

Fig. 2 OM -UVFL mode: a) image of 52.5 cement paste of unaltered sample; b) Reference unaltered sample: cement mortar with dark carbonatic aggregates; major fluorescence activity (bright green) can be observed around aggregates.

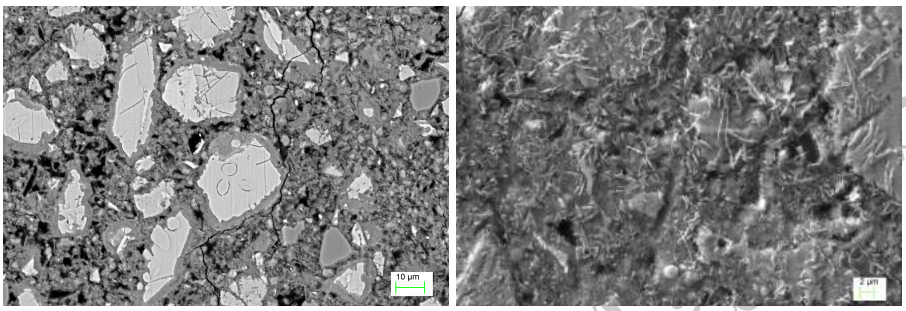

(a) (b)

Fig. 3 SEM images of cement matrix of unaltered reference sample. a) Bright phases of Calcium Alluminate Hydrates (CAH), Calcium Silicate Hydrate (CSH), light grey crystals of Portlandite, dark gray crystals of Ferric phases (CAFH); b) morphological feature of a cement paste with crystals of hydrate minerals.

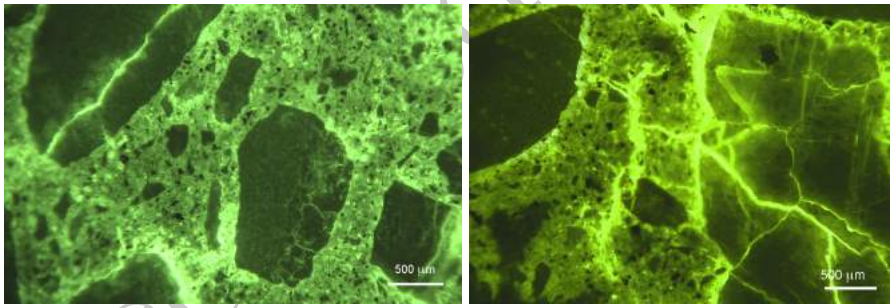

(a) (b)

Fig. 4 UVFL observations of thermal damaged concrete: pervasive microcracks and detachment in the transition zone: a) Thermal treatment 300°C; b) Thermal treatment 600°C.

Please cite this document as: Meloni P., Mistretta F., Stochino F., Carcangiu G. Thermal Path Reconstruction for Reinforced Concrete Under Fire, Fire Technology, 55, 1451-1475, (2019)

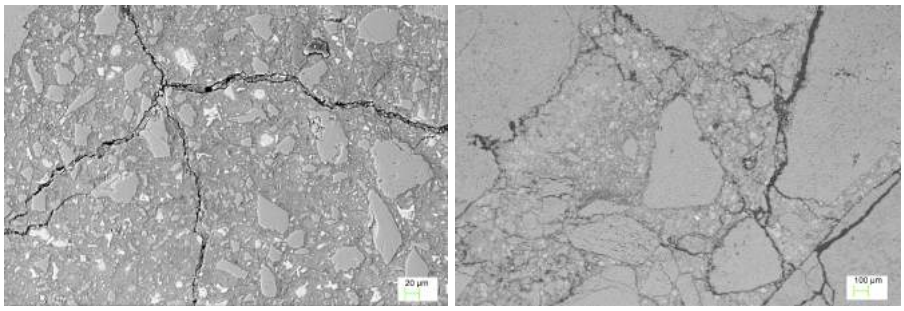

(a) (b)

Fig. 5 SEM Microstructure of thermal damaged concrete: a) Pervasive cracking of the cement matrix; debonding in the interfacial zone (temperature about 400°C); b) Detachement, pulverization, granular disintegration, (temperature about 800°C).

visible effects. It is possible to observe a general discoloration of the cement paste and concrete aggregates (Figure 6) and to see the fractured and debonding system which determines an increase in the porosity of the material that causes an increase in the porosity and a strong loss of mechanical properties [29] of the material.

In cement mortars with limestone aggregates at temperatures $\geq$ 200°C small microcracks, even branched, characterized by submicrometric width, are observed. They tend to stop on the surfaces of the aggreates. At 400°C the level of microfracturing intensifies significantly in the cement matrix, in relation to the dehydration and withdrawal processes, see Figure 6. Microfractures are present not only in the cement matrix but also in the matrix-aggregate transition zone. The cracks opening reaches 6$\div$ 10μm. At 600°C, microfracturing is pervasively extended to the interfaces between the cement matrix and the aggregates: often also the interior of the clasts are fractured. In this case the cracks opening reaches about 20 μm. At higher temperatures, along with the decarbonation processes, the cementitious matrix and the carbonate clasts are consumed. They are detached by pulverization, and fractures are spread with characteristic opening sizes even higher than 100 μm. The specimen made of cement paste suffered more consistent damage with increasing temperatures, exhibiting a different micro-fracturing pattern, characterized by pseudo-linear fracture of an important width. Obviously, the absence of aggregates did not allow the fracture propagation into the interfaces. Therefore, the microscopic observation (OM and SEM) allowed to highlight the evolution of the crack pattern with the increase in temperature and the relative damage suffered by the material. SEM microscopy also allowed to verify the presence of certain mineralogical phases (eg portlandite) and the modifications of the specific surface of the concrete caused by heat exposure. In particular, as the temperature increase the hydrated cement compounds tend to modify the characteristic fibrous-foliated structure by losing the water until the complete dehydration occurs, for the hydrated aluminates, at temperatures close to 500°C [51]. Also the morphology of the thermally treated compounds, the variation of the specific surface and the cracking framework can indicate the achievement of certain temperature [54], [55], [56], [57],

Please cite this document as: Meloni P., Mistretta F., Stochino F., Carcangiu G. Thermal Path Reconstruction for Reinforced Concrete Under Fire, Fire Technology, 55, 1451-1475, (2019)

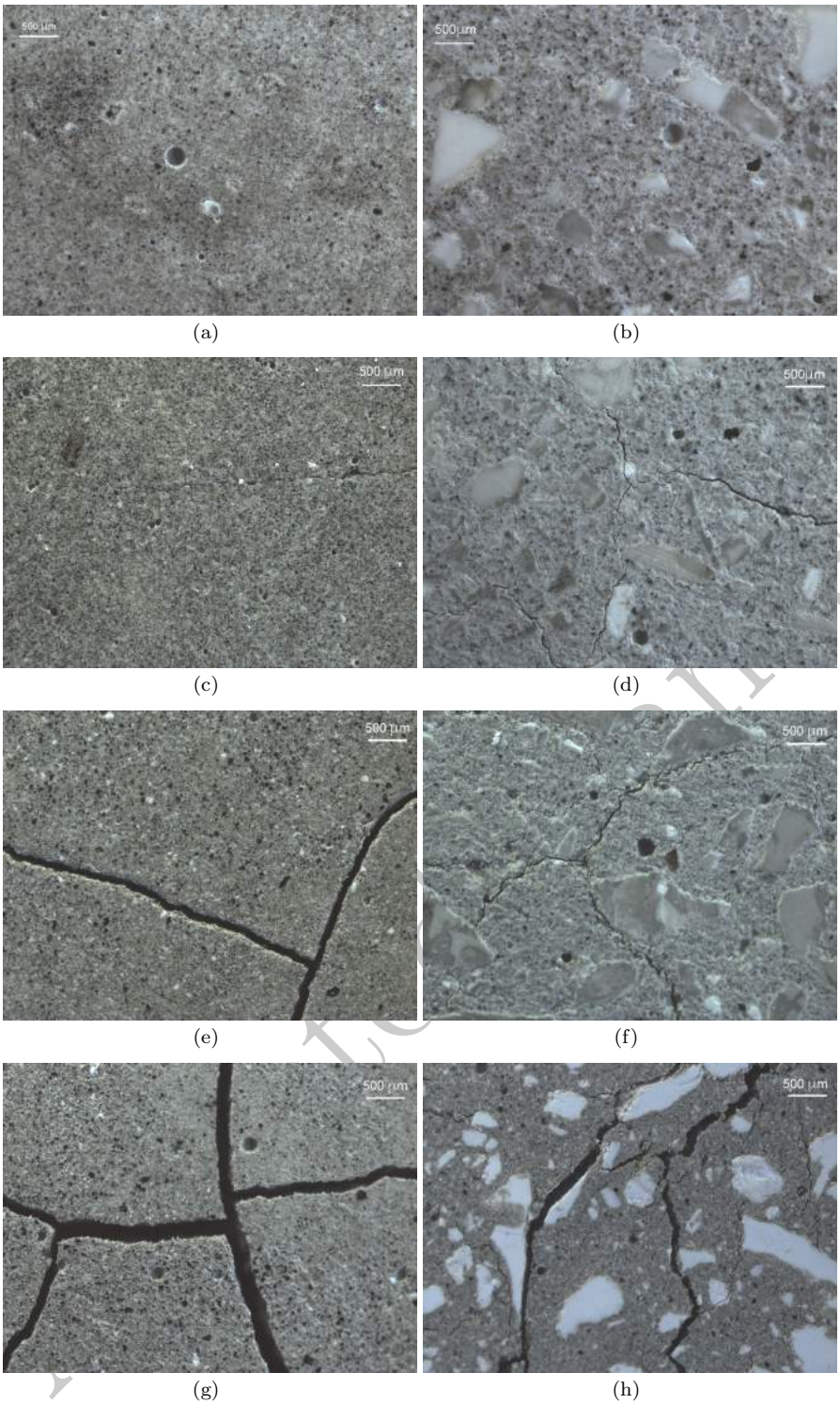

Fig. 6 RL mode observations of thermal damaged cementitious paste (Left) and cementcious mortars with carbonatic aggregates (Right): at 200°C: very slight damage (a,b); 400°C: Microfractures in the cement paste and light discoloration; (c, d). 600°C: severe microcracks on the cementitious paste; development of network of pervasive microfractures and chromatic alteration of cement mortar (e, f). 800°C: very severe fracturation in the cement matrix; complete debonding of aggregates, decarbonation, increase of porosity, polverization and cromatic alteration with brightening of the aggregates

Please cite this document as: Meloni P., Mistretta F., Stochino F., Carcangiu G. Thermal Path Reconstruction for Reinforced Concrete Under Fire, Fire Technology, 55, 1451-1475, (2019)

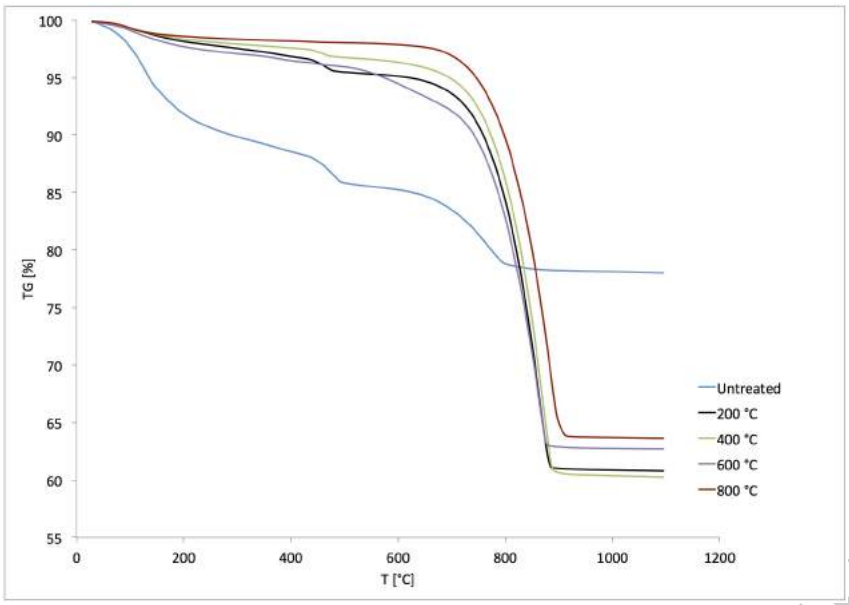

(a)

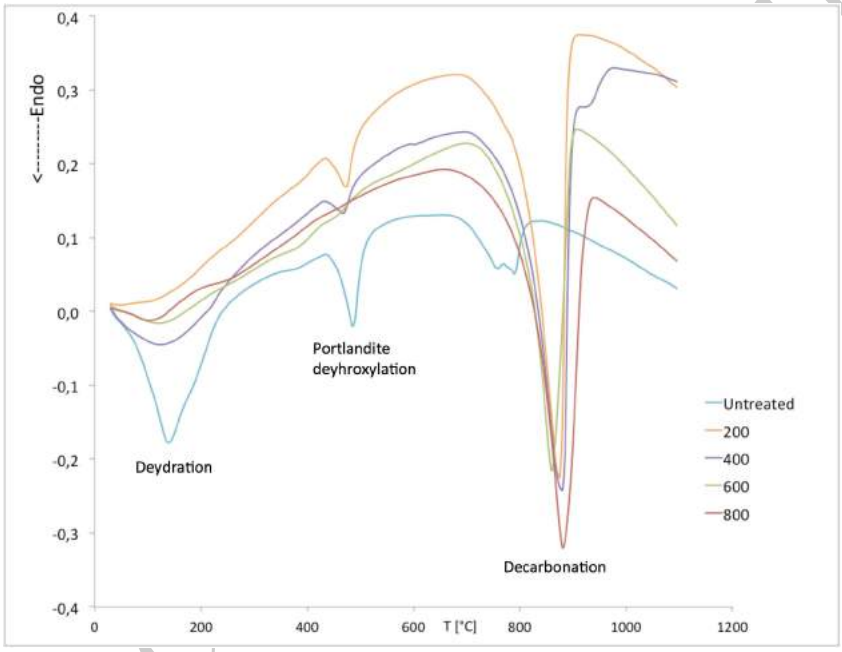

(b)

Fig. 7 Typical multiplot of TG-DTA curves for the considered samples: (a) TG analysis, (b) DTA analysis.

Please cite this document as: Meloni P., Mistretta F., Stochino F., Carcangiu G. Thermal Path Reconstruction for Reinforced Concrete Under Fire, Fire Technology, 55, 1451-1475, (2019)

3.2 XRD TG DTA analysis

In order to assess changes in the mineralogical composition of samples caused by the increase of temperature, XRD and TG-DTA analyses were carried out. In the unaltered reference sample the X-Ray pattern exhibits the presence of Ettringite, Portlandite, Calcite, Dolomite[49], [50]. Portlandite disappears in highly damaged samples [51] exposed to temperatures near and above the 500°C (dehydroxylation reaction of $Ca(OH)2 \Longrightarrow CaO$ occurs in the range $480 \div 500$°C).

Actually, the solid state reactions are influenced not only by the increase in temperature but also by the diffusivity of the gases that can modify the dehydration kinetics of Ca and Mg hydroxides and the rehydration of their oxides [5].

At higher temperature calcium carbonate of the aggregates of the cement-base samples has been transformed into relative oxides; particularly CaO was subject to rapid hydration giving neogenic Portlandite. Primary Portlandite appears in all samples exposed to temperatures lower than 500°C [52], whereas Ettringite is visible in diffraction patterns of undamaged samples because this phase begins to lose bonding water at 80°C [51], [53]. TG-DTA analyses better defined the damage framework by providing indications on the evolution of some thermal effects monitoring amorphous cement phases not detectable using X-Ray Diffraction. A typical thermogram of the cement matrix of undamaged sample is depicted in Fig. 7 with a well definied endothermic peak at 120°C linked to the water loss start by CHS and CAH gels (deydratation and loss of bonded water) [51], [18], [53]. Actually, the CSH and CAH gels in hydrated cement paste consist of very small poorly cristalline structures with disordered layers [51]-[18]-[55]. Some water molecules are absorbed in the interlayer space, other surrounding the external gels structures and water is also present into the capillary pores. The loss of water is a multistep reaction and water molecules require different energy to be released. Absorbed and monolayer water molecules, that surround gel structures, are released at first. The interlayer water molecules are more bounded and then could be released at higher temperature. A sharp endothermic peak at about 500°C is related to the Portlandite occurrence. At about 700°C, decarbonation processes began to start and a complete transformation in Mg and Ca oxide takes place at the 770-895°C range with a significant and well defined endothermic peak when carbonatic aggregates were present. In thermograms (Figure 7) referred to samples exposed to a temperature higher than 600°C Portlandite is absent; it can be found as secondary phase (P*) due to a rehydration process of the CaO. A slight endothermic effect can be seen at about 780°C. It corresponds to the first dolomite decarbonation step while a complete decarbonation occurs at about 900°C. A typical thermogram of a strongly damaged sample usually displays the peak of decarbonation, unless it contains secondary Portlandite, which reaches its endothermic peak at lower temperatures, from 20° to 50°C, different from the expected level of 490°C. This thermal shift is well described in [52].

3.3 MIP Porosimetry

Porosimetric measures were carried out for cement pastes, Figure 8 - Table 1, and cement mortars samples, Figure 9 - Table 1, containing fine carbonatic sand, exposed to heat at selected temperatures. The pore size distribution of thermal

Please cite this document as: Meloni P., Mistretta F., Stochino F., Carcangiu G. Thermal Path Reconstruction for Reinforced Concrete Under Fire, Fire Technology, 55, 1451-1475, (2019)

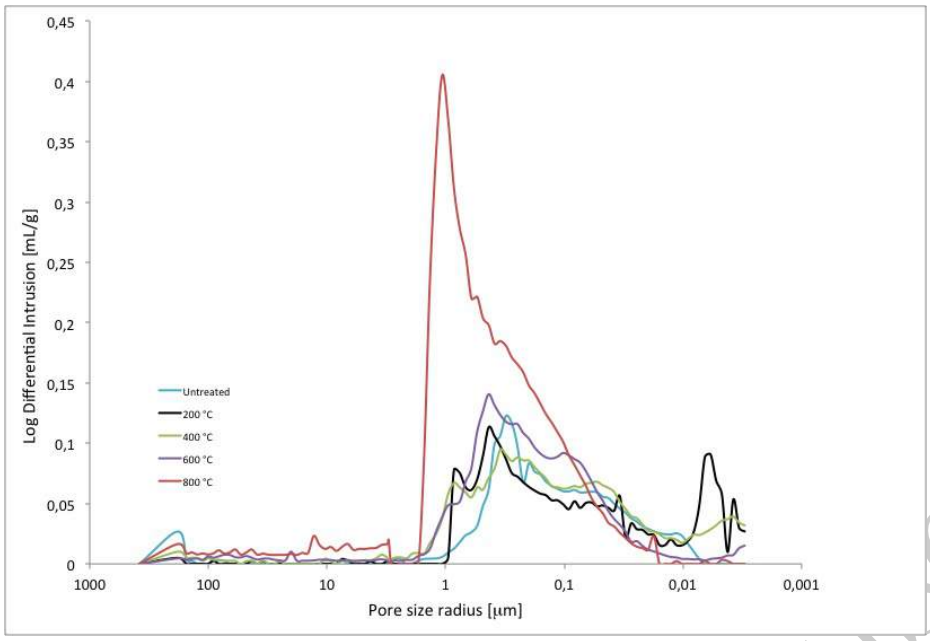

Fig. 8 Multiplot of porosimetric distribution of untreated and thermal treated cement pastes

untreated cement pastes is in the range of about 2.00÷0.007 μm, (modal pore radius equal to 0.30 μm), see Figure 8 and Table 1. The heat exposure causes a significant change in the porous microstructure ([19], [58], [59],[60], [61], [62], [63]); at 100 ÷ 200 °C drying processes are dominant and particularly at 180°C bound water starts to be released accompanied by a loss of mass (of about 8 %). A new class of voids of small radius (< 0.01μm gel pores) appears as a consequence. Also porosimetric curve of the sample treated up to 400°C exibits an increase of pores of radius smaller than 0.01μm and a simultaneous increase of those larger of 0.5 μm (the average radius shifts towards micropores of about 0.06 μm). The first effect can be still related to the interstratified water loose from the cement hydrates gels.

The cement paste heated up to 600°C exhibits a significative increase of porosity, due to Portlandite depletion and severe microcacking occurence; the pore size distribution ranges from 0.01÷2 μm shifting versus much larger pores while interstitials submicrometric pores seem to collapse see Table 1. At 800°C the porosimetric distribution exhibits a sharp shift (range of 0.1÷3 μm) versus large pore and the total porosity becomes very high [64], see Table 1. For the cement mortars, Figure 9, the pore size distribution tends to became gradually bimodal rising the temperatures. Capillary pores generally exhibit a dimension of about 1 μm while the gel pores have a radius shorter than 0.01μm (see [60]). The porogram of untreated mortars (Figure 9) shows similar characteristics of those of cement pastes with a sharp narrow peak at 1.5 μm due to the presence of capillary voids. The heat exposure causes the depletion of absorbed, bonded, interstitial gel water [51] and therefore pores of radius lower than 0.01μm (gel pores) appear up to 400°C. At 600°C the distribution changes and shifts versus large pores (aver-

Please cite this document as: Meloni P., Mistretta F., Stochino F., Carcangiu G. Thermal Path Reconstruction for Reinforced Concrete Under Fire, Fire Technology, 55, 1451-1475, (2019)

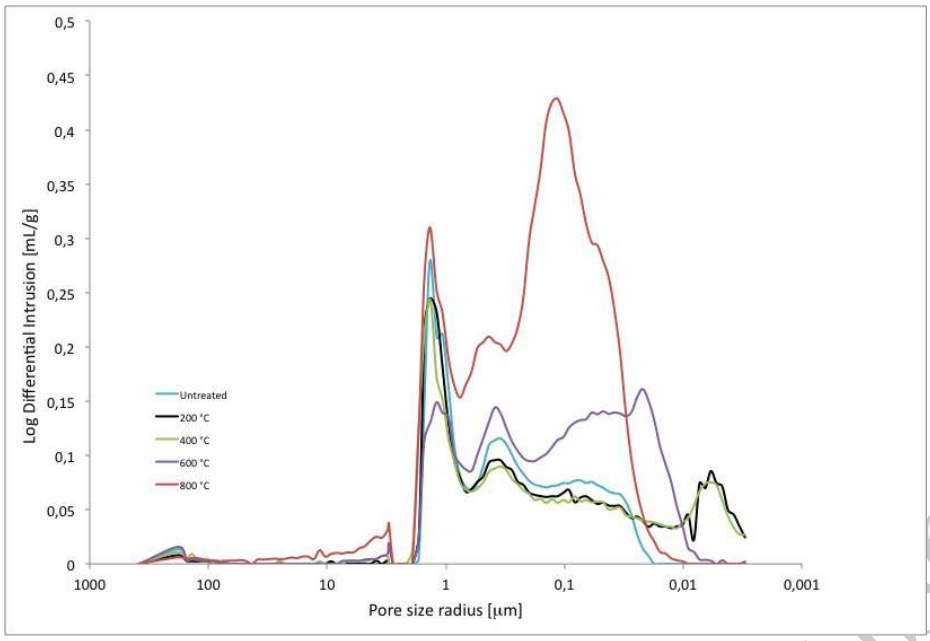

Fig. 9 Typical multiplot of porosimetric distribution of untreated and thermal treated cement mortars

Table 1 Summary of Porosity Measures

Sample	Cement Pastes		Cement Mortars	
	MIP Open Porosity (%)	MIP Total Porosity (%)	MIP Open Porosity (%)	MIP Total Porosity (%)
Untreated	28.8% ± 0.7	28.7% ± 0.7	28.0% ± 0.9	28.0% ±1.9
TT200°C	38.7% ± 1.4	38.7 % ± 1.4	37.2% ± 1.9	37.2% ±1.8
TT400°C	33.1% ± 2.9	33.1 % ± 2.9	32.0% ± 2.6	32.0% ±2.6
TT600°C	43.6% ± 2.3	43.6 % ± 2.3	42.2% ± 3.3	42.2% ±3.2
TT800°C	53.8% ± 3.5	53.8 % ± 3.6	55.4% ± 3.9	55.4% ±3.9

age radius about 0.06 μm) and the total porosity exceeded the values of 40% due to debonding at the interfaces cement matrix-aggregates, diffuse microcraks and Portlandite depletion. At 800°C the porosity higher than 55% was strongly influenced by decarbonation processes and by very severe cracking and pulverization of the cement-base materials that completely loose physical-mechanical performances [29], [64], [65], [66], [67].

3.4 Colorimetry

A set of color measurements were carried out on heated samples in order to develop a reference scale to identify temperatures capable of modifing the colour of the concrete different components. This can be useful in order to detect such

Please cite this document as: Meloni P., Mistretta F., Stochino F., Carcangiu G. Thermal Path Reconstruction for Reinforced Concrete Under Fire, Fire Technology, 55, 1451-1475, (2019)

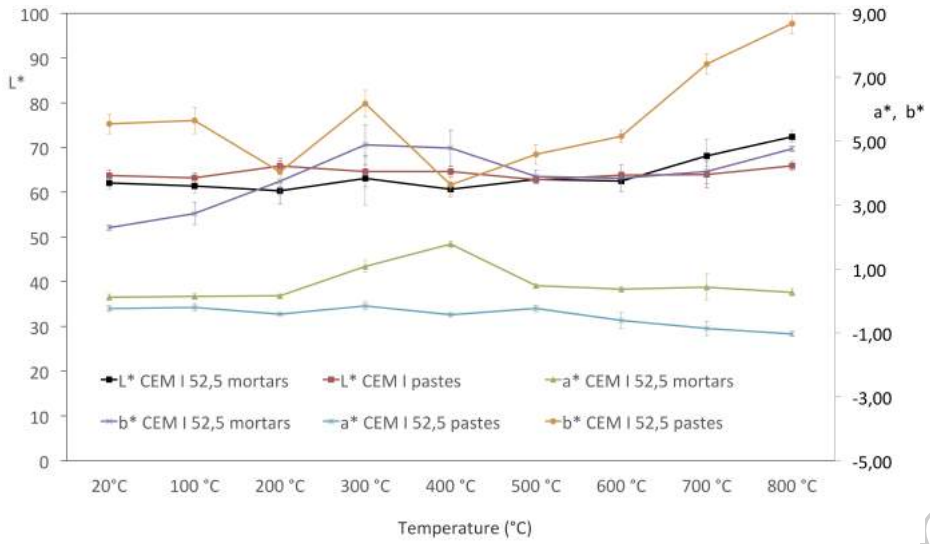

Fig. 10 Colorimetric values of a*, b* and L* (CIE Lab 76 colour space) for cement mortars and cement 52.5 pastes (CEM I 52.5 R) heat exposed. Standard deviation bars are also presented for each case.

modifications even in case of real fire when it is important to have an easy and quick assessment of the peak temperatures, see [12], [23], [68], [69].

Fig. 10 shows the variations of the chromaticity coordinates a*, b* and L* (CIE Lab 76 colour space see [13]) for both the cement matrix of concrete and for cement only (CEM I 52,5 R) from a room temperature up to 800°C. Instead, Fig. 11 illustrates the chromatic variations on originally beige-pinkish aggregates.

Carbonate sand is the chromatically sensitive component while the cement paste alone (CEM I 52,5 R) does not display significant color changes in the considered thermal range [70], [71]. A slight increase in the a* and b* values (reddening, yellowing, lightening) in the 300-400°C, thermal range can be due to the behavior of the carbonate material. The L* value and occasionally the b* value can increase at temperatures exceeding 700°C. Instead, the single aggregates [72] provide objective and reliable indications on the reached temperatures. Two thermal ranges are the most significant: the first one between 300-400°C leading to a reddening, yellowing or browning of the components containing Fe, due to the oxidation of FeO- OH to -Fe2O3. At 500°C these effects decrease and at 600°C they are negligible.

Assessing the temperature corresponding to the reddening is very important because it identifies the parts of concrete which present a significant reduction in the mechanical characteristics [9], [24], [29], [46]. Starting from 700°C, a strong lightening becomes evident, with a relevant increase in the L* values, especially in case of carbonated components at the beginning of a decarbonation process, see also Figure 6.

An interesting synthesis of these results can be found in Table 2 which presents the most important diagnostic features of concrete exposed to heating. The location of these features in real cases allows a better understanding of the thermal

Please cite this document as: Meloni P., Mistretta F., Stochino F., Carcangiu G. Thermal Path Reconstruction for Reinforced Concrete Under Fire, Fire Technology, 55, 1451-1475, (2019)

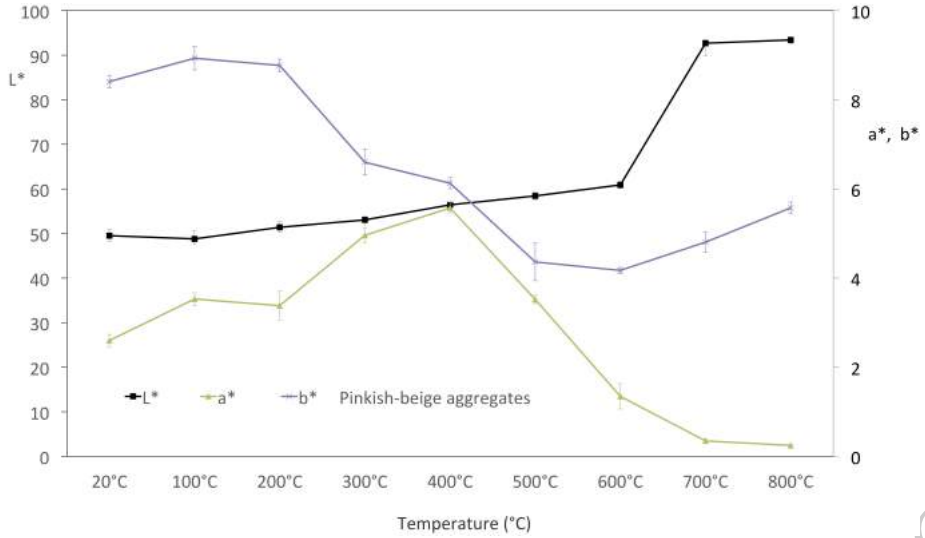

Fig. 11 Colorimetric values (a*, b* and L*; CIE Lab Colour Space) for pinkish-beige carbonatic aggregates heated up to 800°C. Standard deviation bars are also presented for each case.

event and a suitable design in terms of demolition and reconstruction works of damaged structures.

Table 2: Summary of diagnostic features and mechanical changes in concrete caused by fire exposure see [8] - [46] -[47] - [66] - [68], [70] - [71] - [73] - [74] - [75] - [76])

T °C	**XRD and TG-DTA**	**MIP Porosimetry**	**Colorimetry**	**Strength Changes**
70÷80	Dissociation of ettringite			
≤ 150	In the range 30÷150°C a quick weight loss of the evaporable-free water and part of the physically bound water of hydrate CSH gels can be observe. Endothermic effect discriminable starting at about 120°C.	The deydratation favour the onset of microcracking and a slight increase of porosity in the cement matrix.		Minor loss of strength possible (<10%)

Please cite this document as: Meloni P., Mistretta F., Stochino F., Carcangiu G. Thermal Path Reconstruction for Reinforced Concrete Under Fire, Fire Technology, 55, 1451-1475, (2019)

Table 2: Summary of diagnostic features and mechanical changes in concrete caused by fire exposure see [8] - [46] -[47] - [66] - [68], [70] - [71] - [73] - [74] - [75] - [76])

T °C	**XRD and TG-DTA**	**MIP Porosimetry**	**Colorimetry**	**Strength Changes**
120÷175	Dissociation of gypsum, causing its depletion in the cement paste. Dehydroxylation of gypsum with formation of alpha hemihydrate at 163°C. Water loss from Calcium Carboalluminates. Endothermic peak at about 175°C		Very slight cromatic changes.	
235	Water loss from hydrate tetracalcic alluminate. Endothermic peak at 235°C	MIP technique clearly reveals the presence of small pores of radius < 0.01 μm (gel pores).		
>300	Loss of bound water in cement matrix and associated degradation become more prominent. Dehydroxylation of brucite Mg(OH)2. Endothermic peak at about 388°C.	Small pores of radius < 0.01 μm (gel pores) are yet evident in the pore size distribution. Increase in open porosity with values exceeding 30%. At temperatures exceeding 400°C gel pores structure almost disappear and pore size distribution shifts versus smaller voids up to capillary ones (pore radius $>1\mu$m).	Changes in colour became more evident specially to mineralogical phasese containing cromophorous elements (e.g. Fe, Mn, Ni, etc).	Marked increase in micro-cracking. Significant loss of strength starts at 300°C
300÷350	Oxidation of FeO-OH to α-Fe2O3		Clear change in colour to pink or reddish brown of aggregates	Detachement of particles sand in size.
573	5% increase in volume of quartz (from phase α to β transition) causing radial cracking around quartz grains. Endothermic peak at about 491°C			

Please cite this document as: Meloni P., Mistretta F., Stochino F., Carcangiu G. Thermal Path Reconstruction for Reinforced Concrete Under Fire, Fire Technology, 55, 1451-1475, (2019)

Table 2: Summary of diagnostic features and mechanical changes in concrete caused by fire exposure see [8] - [46] -[47] - [66] - [68], [70] - [71] - [73] - [74] - [75] - [76])

T °C	**XRD and TG-DTA**	**MIP Porosimetry**	**Colorimetry**	**Strength Changes**
450÷500	Dehydroxylation of Portlandite, Endothermic peak at about 491°C.	The mineralogical change causing Portlandite depletion in the cement paste yet increase the total porosity.	The reddish-brown color gradually fades.	
600÷800	Release of carbon dioxide from carbonates may cause considerable contraction of the concrete. Early decarbonation of dolomite occur, first step: 750°÷800°C.	Porosity exceeds values of the 40%. A sharp shift of the dimensional pore size distribution versus smaller pores can be observed.	Carbonatic aggregates become very whites starting from 750°C. Cement matrix tends to became more clear assuming a slight beige colour.	Severe microcracking of the cement matrix and aggregates. Decisive reduction of concrete strength for heating at temperatures beyond of 500÷600°C
800÷1200	Decarbonation of dolomite, (second step): 850°÷950°C. Decarbonation of calcite, endothermic peak at about 895°C. Dissociation and extreme thermal stress cause complete disintegration of calcareous constituents, resulting in whitish-grey concrete colour and severe microcracking. Concrete starts to melt at about 1200°C.	At 800°C a large amount of pores of about 0.1μm appeared in the porogram. The total porosity exceeds 50% for mortars and concrete containing carbonatic aggregates.		

4 Conclusions

4.1 Remarks

The structural assessment of concrete exposed to fire can be a very difficult task. In this paper, several methods were applied to assess the materials damages and modifications due to the temperature variation.

Cement paste is generally composed of 50-60% C-S-H, 20-25% CH and other chemical phases, such as ettringite, monosulfate, and unhydrated cement compounds. The aggregates occupy about 65 ÷ 75% of the concrete volume. The

Please cite this document as: Meloni P., Mistretta F., Stochino F., Carcangiu G. Thermal Path Reconstruction for Reinforced Concrete Under Fire, Fire Technology, 55, 1451-1475, (2019)

concrete behavior, particularly at elevated temperatures, is largely affected by the mineralogical composition of aggregates. The duration of the heating and the heating rate can influence the chemical modifications of the constituents. The most important chemical reactions are related to the dehydration of compounds such as CSH and CAH [51], to dehydroxylation of hydroxides [77], [78], to decarbonation and to the appearance of new phases for partial sintering or melting. Many reactions are linked to the specific chemical nature of the aggregates and any additives. The phase transition of α-quartz to β-quartz was at 575°C, associated to a volume increase, is very important for the material degradation. Each of these transformations, under a sub-solidus regime, is conditioned by numerous factors, including the duration of the thermal event [51], [79], [80], [81], [82], [83], [84]. For example, for a normal concrete, exposed to 300°C, 600°C and 900°C for 1,2,3, 6 and 9 hours, the residual strength decreases continuously as the temperatures increase: the longer the exposure time the more the resistance is reduced. However, is the thermal peaks that produces the most consistent degradation effects.

4.2 Outcome

Experimental investigations have been carried out on cement pastes and mortars with carbonate aggregates. XRD, TG-DTA, MIP, OM and SEM analyses, along with colorimetric investigations, have provided useful indications regarding the temperatures reached by the fire-exposed concrete, based on changes in mineralogical composition and microstructure.

The cracking system (e.g. wide, length, areal frequency, etc.) can be correlated to the material damage and to the temperature time-history. Indeed the crack pattern is augmented by temperature surge. The presence of the carbonate sandy aggregate, within 500 °C, prevented the propagation of microcracks since the fracture energy was consumed at the matrix/aggregate interfaces. Vice versa, cementitious paste are more intensively fractured, with pseudo-linear fractures of considerable width (e.g. about 70 μm at 600 °C against 20 μm for the cement mortars). The quantification of the defects, through microscopic observations and image analysis, can allow to define the degree of concrete damage (areal persistence and intensity of fractures per unit of surface).

Portlandite plays a key role in determining the reached temperatures. The absence of this phase, caused by its dehydroxylation, indicates a temperature of about 500 °C. Therefore, isotherms could be traced in a fire scenario using the presence of Portlandite to distinguish zones exposed up to 500 °C and more. The lowering of the de-hydroxylation temperature of Portlandite can be interpreted as an indicative factor for the presence of secondary neogenic Portlandite. This mineral could be derived by the hydration of CaO due to decarbonatation process at temperatures range of 800÷950 °C.

MIP investigations provide useful information about CSH and CAH gel damage. The increase of capillary pores and the collapse of gel pores allowed to discriminate temperature effects up to 400°C. At 200 °C a peak around 0.01 μm, due to the first step of dehydration, is clearly visible in the pore size distribution. At 400 °C this effect results less pronunciated and disappears at 600°C. In the case of cement mortars, the open porosity significantly increased up to 42% and 55% at 600°C and 800°C respectively, due to strong debonding, microfracture,

Please cite this document as: Meloni P., Mistretta F., Stochino F., Carcangiu G. Thermal Path Reconstruction for Reinforced Concrete Under Fire, Fire Technology, 55, 1451-1475, (2019)

decarbonation of aggregates. At each porosity modification, induced by thermal treatment, a corresponding severe loss of mechanical strength and durability were assessed.

Colorimetric investigations on artificially thermal treated samples were useful to recognize the most significative chromatic alterations caused by heat exposure. Particularly, two chromatic changes occur at definite temperature ranges; a first causing the reddening of original pinkish-beige aggregates in the 300-400 °C range and a second one a considerable lightening of concrete starting from approximately at 700 °C. The information resulting from the use of instrumental techniques provided some significant markers for the definition of isotherms: disappearance of ettringite at about 80°C, deydratation of cement paste in the range 200÷400°C, oxidation of FeO-OH into α-Fe_2O_3 at 300-400°C, Portlandite deydrossilation at 500°C, a significant variation in the pore size distribution with a strong increase of porosity at 600°C, start of decarbonation of $CaMgCO_3$ and $CaCO_3$ at 750°C with a strong increase of porosity, fracturing and lightening with high L* values. The possibility of detecting the mineralogical and physical transformations of the concrete subjected to heat, also using laboratory samples thermally degraded, allows to get cognitive tools useful to the zoning of an area affected by fire and so distinguish the areas less damaged from those critical ones. This is useful in the assessment phase of the conservation status of the building and planning of interventions for demolition, recovery and repair. These studies can be useful also in the temperatures setting to be included in fluodynamic modeling programs targeted to reconstruct the real fire scenario.

It is also important to underline that also Differential Scanning Calorimetry, or DSC, can be useful to determine the thermal path benchmarks. Unfortunately the authors could not perform this analysis during the experimental campaign but it is reccomendend for future studies.

Finally further developments of this research are expected considering different concrete mixes and different temperature gradients. Indeed it would be interesting to study the effects of high heating rates that can be achieved during real fire incidents.

Acknowledgements The financial support of the Italian Ministry of University and Research, the Conference of Rectors of Italian Universities and Confindustria, the Italian Industrial Federation, under the PhD-ITalents programme grant n. 145145711

References

1. Gales J., Parker T., Cree D., Green M. (2016). Fire Performance of Sustainable Recycled Concrete Aggregates: Mechanical Properties at Elevated Temperatures and Current Research Needs. Fire Technology 52: 817-845.
2. Anand N, Prince G. (2014). Effect of Grade of Concrete on the Performance of Self-Compacting Concrete Beams Subjected to Elevated Temperatures. Fire Technology 50: 1269-1284.
3. Del Prete I., Bilotta A., Nigro E. (2015) Performances at high temperature of RC bridge decks strengthened with EBR-FRP. Composites Part B: Engineering 68. 27-37.
4. Nigro E., Bilotta A., Cefarelli G., Manfredi G., Cosenza E. (2012). Performance under fire situations of concrete members reinforced with FRP rods: Bond models and design nomograms. Journal of Composites for Construction 16: 395-406.

Please cite this document as: Meloni P., Mistretta F., Stochino F., Carcangiu G. Thermal Path Reconstruction for Reinforced Concrete Under Fire, Fire Technology, 55, 1451-1475, (2019)

5. Lamond J.F,Pielert J.H. (2006) Significance of Tests and Properties of Concrete and Concrete Making Materials, ASTM, International-Standars Wordwide, STP 196 D, Bridgeport, NJ.
6. Overholt K.J., Ezekoye O.A. (2015). Quantitative Testing of Fire Scenario Hypotheses: A Bayesian Inference Approach. Fire Technology 51: 335-367.
7. Östman B., Tsantaridis L. (2015). Fire Scenarios for Multi-storey Façades with Emphasis on Full-Scale Testing of Wooden Façades. Fire Technology 51:1495-1510.
8. Annerel E., Taerwe L. (2009). Revealing the temperature history in concrete after fire exposure by microscopic analysis. Cement and Concrete Research 39: 1239-1249.
9. Nijland T.G., Larbi J.A. (2001). Unravelling the temperature distribution in fire-damaged concrete by means of PFM microscopy: Outline of the approach and review of potentially useful reactions. Heron 46: 253-264.
10. Hurley J.M., Gottuk D., Hall J.R., Harada K., Kuligowski E., Puchovsky M., Torero J.L., Watts J.M., Wieczorek C.J., SFPE Handbook of Fire Protection Engineering, Springer, (2015).
11. Li M., Qian C.X., Sun W. (2004). Mechanical properties of high-strength concrete after fire. Cement and Concrete Research 34: 1001-1005.
12. Colombo M., Felicetti R. (2007). New NDT techniques for the assessment of fire-damaged concrete structures. Fire Safety Journal 42: 461-472.
13. Stochino F., Mistretta F., Meloni P., Carcangiu G. (2017) Integrated approach for post-fire reinforced concrete structures assessment, Periodica Polytechnica Civil Engineering 61(4): 677-699.
14. Acito M., Stochino F., Tattoni S. (2011). Structural response and reliability analysis of RC beam subjected to explosive loading. Applied Mechanics and Materials, 82: 434-439.
15. Stochino F. (2016). RC beams under blast load: Reliability and sensitivity analysis. Engineering Failure Analysis, 66: 544-565.
16. Hollis, N.W. (1999). Petrographic Methods of Examining Hardened Concrete: A Petrographic Manual. Technical report VTRC-92-R14, Virginia Transportation Research Council (VTRC).
17. Ramachandran V.S., Beaudoin J.J. (2001). Handbook of Analytical Techniques In Concrete Science And Technology, Principles, Techniques, and Applications. Noyes Publications, William Andrew Publishing, LLC Norwich, New York, NY. 2001.
18. Taylor H.F.W., Beaudoin J.J. (1964). The Chemistry of Cements. Academic Press Inc., London, UK. 1964.
19. Pei Y., Agostini F., Skoczylas F., (2017). The effects of high temperature heating on the gas permeability and porosity of a cementitious material. Cement and Concrete Research, 95:141-151.
20. Sant G., Bentz D., Weiss J. (2011). Capillary porosity depercolation in cement-based materials: Measurement techniques and factors which influence their interpretation. Cement and Concrete Research 41, 8:854-864.
21. Herve E., Care S., Seguin J.P.(2010). Influence of the porosity gradient in cement paste matrix on the mechanical behavior of mortar. Cement and Concrete Research, 40,7,1060-1071.
22. Bazant Z.P., M.F. Kaplan Concrete at High Temperatures. Longman Addison-Wesley, London (1996).
23. Hager I. (2014). Colour Change in Heated Concrete, Fire Technology. 50: 945-958.
24. Yüzer N., Aköz F., Öztürk L.D. (2004). Compressive strength-color change relation in mortars at high temperature. Cement and Concrete Research. 34(10): 1803-1807.
25. Kirchhof L.D., Lorenzi A., Silva Filho L.C.P. (2015). Assessment of Concrete Residual Strength at High Temperatures using Ultrasonic Pulse Velocity. The e-Journal of Nondestructive Testing, 20(7): 1-9.
26. Lin C.H., Chen S.T., Hwang T.L. (1989). Residual strength of reinforced concrete columns exposed to fire. Journal of the Chinese Institute of Engineers, 12(5), 557-566.
27. Lie T.T., Rowe T.J., Lin T.D. (1986). Residual strength of fire-exposed reinforced concrete columns. Special Publication, 92, 153-174.
28. Chen X., Wu S., Zhou J. (2013). Influence of porosity on compressive and tensile strength of cement mortar. Construction and Building Materials, 40, 869-874.
29. Bahr O., Schaumann P., Bollen B., Bracke J., Young's modulus and Poisson's ratio of concrete at high temperatures: Experimental investigations, Materials and Design, Elsevier (2012).

Please cite this document as: Meloni P., Mistretta F., Stochino F., Carcangiu G. Thermal Path Reconstruction for Reinforced Concrete Under Fire, Fire Technology, 55, 1451-1475, (2019)

30. Mehta P.K, Monteiro, P.J.M (2006). Concrete: Microstructure, Properties and Materials, McGraw-Hill Professional, New York 2006.
31. Brandt, A. M. Cement-based composites: materials, mechanical properties and performance. CRC Press, Taylor and Francis, 2005.
32. Chan Y. N., Peng G.F., Anson M. (1999). Residual strength and pore structure of high-strength concrete and normal strength concrete after exposure to high temperatures. Cement and Concrete Composites, 21(1), 23-27.
33. Kumar R., Bhattacharjee B. (2003). Porosity, pore size distribution and in situ strength of concrete. Cement and concrete research, 33(1), 155-164.
34. Casnedi L., Cocco O., Meloni P., Pia G. (2018) Water Absorption Properties of Cement Pastes: Experimental and Modelling Inspections. Advances in Materials Science and Engineering, article id: 7679131.
35. Pia G., Sanna U. (2013). A geometrical fractal model for the porosity and thermal conductivity of insulating concrete. Construction and Building Materials, 44, 551-556.
36. Mistretta F., Stochino F. (2017) Case study of a reinforced concrete industrial warehouse exposed to fire: Post fire investigation and retrofitting, Proceedings of 2nd International Fire Safety Symposium, Naples June, 7-9, 2017.
37. Mistretta F., Serra A., Stochino F. (2017) Fire on prestressed reinforced concrete: CFD and FE thermo-mechanical simulation, Proceedings of 2nd International Fire Safety Symposium, Naples June, 7-9, 2017.
38. Zhang, B., Cullen, M., Kilpatrick, T. (2016). Spalling of heated high performance concrete due to thermal and hygric gradients. Advances in Concrete Construction, 4(1): 1-13.
39. Dauti, D., Tengattini, A., Dal Pont, S., Toropovs, N., Briffaut, M., Weber, B. (2018). Analysis of moisture migration in concrete at high temperature through in-situ neutron tomography. Cement and Concrete Research, 111: 41-55.
40. Bazant Z.P. (1997), Analysis of pore pressure, thermal stresses and fracture in rapidly heated concrete, Proceedings of International Workshop on Fire Performance of High-Strength Concrete. NIST Spec. Publ. 919, L. T. Phan, N. J. Carino, D. Duthinh, and E. Garboczi, eds., National Institute of Standards and Technology, Gaithersburg, Md., 155?164.
41. Mindeguia J.-C., Pimienta P. , Noumowé A., Kanema, M. (2010) Temperature, pore pressure and mass variation of concrete subjected to high temperature - experimental and numerical discussion on spalling risk, Cement and Concrete Research 40 (3): 477-487.
42. Noumowe A., Carré H., Daoud A., Toutanji H. (2006) High-strength self-compacting concrete exposed to fire test, ASCE Journal of Materials in Civil Engineering 18(6): 754-758.
43. Klingsch E., (2014) Explosive spalling of concrete in fire, IBK-Bericht 356: 1-251.
44. Liu J.C., Tan K.H., Yao Y., A new perspective on nature of fire-induced spalling in concrete, Construction and Building Materials 184: 581-590
45. Gražulis, S., Daškevič, A., Merkys, A., Chateigner, D., Lutterotti, L., Quirós, M., Serebryanaya, N. R., Moeck, P., Downs, R. T., Le Bail, A. (2012). Crystallography Open Database (COD): an open-access collection of crystal structures and platform for world-wide collaboration. Nucleic Acids Research 40, 420-427.
46. Ingham, J.P. (2009). Application of petrographic examination techniques to the assessment of fire-damaged concrete and masonry structures. Materials Characterization 60: 700-709.
47. Georgali B., Tsakiridis P.E. (2005). Microstructure of fire damaged concrete. A case study. Cement and Concrete Composite 27: 255-259.
48. Morgan J. Hurley, Daniel Gottuk, John R. Hall Jr., Kazunori Harada, Erica Kuligowski, Milosh Puchovsky, José L. Torero, John M. Watts Jr., Christopher J. Wieczorek . SFPE Handbook of Fire Protection Engineering, Ed. Springer, 2015.
49. Scrivener KL, Fullmann T, Gallucci E, Walenta G, Bermejo E. Quantitative study of Portland cement hydration by X-ray diffraction/Rietveld analysis and independent methods. Cement and Concrete Researches 34(9):1541-7.
50. Sabeur H., Platret G., Vincent J. (2016). Composition and microstructural changes in an aged cement pastes upon two heating-cooling regimes, as studied by thermal analysis and X-ray diffraction. Journal of Thermal Analysis and Calorimetry 126:1023-1043.
51. Zhang Q., Guang Y. (2012). Dehydration kinetics of Portland cement paste at high temperature. Journal of Thermal Analysis and Calorimetry 110: 153-158.
52. Alarcon-Ruiz L., Plateret G., Massieu E., Ehrlacher A. (2005). The use of thermal analysis in assessing the effect of temperature on a cement paste. Cement and Concrete Research 35: 609-613.
53. Shimada Y, Young JF. (2001). Structural changes during thermal dehydration of ettringite. Advances in Cement Research 13(2):77-81.

Please cite this document as: Meloni P., Mistretta F., Stochino F., Carcangiu G. Thermal Path Reconstruction for Reinforced Concrete Under Fire, Fire Technology, 55, 1451-1475, (2019)

54. Mazars J.(1986). A description of micro- and macro- scale damage of concrete structures. Engineering Fracture Mechanics 25: 729-37.
55. Tantawy M.A. (2017). Effect of High Temperatures on the Microstructure of Cement Paste. Journal of Materials Science and Chemical Engineering 5: 33-48.
56. Fu Y.F., Wong Y.L., Tang C.A., Poon C.S. (2004). Thermal induced stress and associated cracking in cement-based composite at elevated temperatures-Part I: Thermal cracking around single inclusion. Cement and Concrete Composites 26: 99-111.
57. Fu Y.F., Wong Y.L., Tang C.A., Poon C.S. (2004). Thermal induced stress and associated cracking in cement-based composite at elevated temperatures-Part II: thermal cracking around multiple inclusions. Cement and Concrete Composites 26: 113-126.
58. Zadražil T., Vodák F., Kapičková O. (2004). Effect of Temperature and Age of Concrete on Strength – Porosity Relation. Acta Polytechnica, 44:53-56.
59. Ye G., Liu X., De Schutter G., Poppe A.M., Taerwe L. (2007). Influence of limestone powder used as filler in SCC on hydration and microstructure of cement pastes. Cement & Concrete Composites 29: 94-102.
60. Zhang Q.,Ye G. (2011). Microstructure Analysis of Heated Portland Cement Paste. Procedia Engineering 14: 830-836.
61. Cnudde V., Cwirzen A., Masschaele B., Jacobs P.J.S. (2009). Porosity and microstructure of building stones and concretes. Engineering Geology 103: 76-83.
62. Casnedi L., Cocco O., Meloni P., Pia G. (2017). Water absorption properties of cement pastes: Experimental and modelling inspections. Advances in Materials Science and Engineering. Accepted for publication.
63. Gawin D., Pesavento F. (2012). An Overview of Modeling Cement Based Materials at Elevated Temperatures with Mechanics of Multi-Phase Porous Media. Fire Technology 48: 753-793.
64. Mendes A., Sanjayan J.G., Gates W.P., Collins F. (2012). The influence of water absorption and porosity on the deterioration of cement paste and concrete exposed to elevated temperatures, as in a fire event. Cement and Concrete Composites, 34: 067-1074.
65. Ghan Y. N., Peng G. F., Anson M. (1999). Residual strength and pore structure of high-strength concrete and normal strength concrete after exposure to high temperatures. Cement and Concrete Composites 21: 23-27.
66. Chan Y.N., Luo X., Sun W. (2000). Compressive strength and pore structure of high-performance concrete after exposure to high temperature up to 800° C. Cement and Concrete Research, 30(2): 247-251.
67. Chan YN, Luo X, Sun W. (2000). Compressive strength and pore structure of high performance concrete after exposure to high temperature. Materials and Structures 33: 294-298.
68. Annerel E., Taerwe L. (2011). Methods to quantify the colour development of concrete exposed to fire. Construction and Building Materials 2: 3989-3997.
69. Short N.R., Purkiss J.A., Guise S.E (2011). Assessment of fire-damaged concrete using colour image analysis. Construction and Building Materials 15: 3-15.
70. Handoo S.K., Agarwal S., Agarwal S.K. (2002). Physicochemical, mineralogical, and morphological characteristics of concrete exposed to elevated temperatures. Cement and Concrete Research 32(7): 1009-1018.
71. Jinwoo A., Sonny Kim S., Nam B.H., Durham S.A. (2017). Effect of Aggregate Mineralogy and Concrete Microstructure on Thermal Expansion and Strength Properties of Concrete. Applied Sciences 7(12) n. 1307.
72. Xing Z., Beaucour A.L., Hebert R., Noumowe A., Ledesert B. (2011). Influence of the nature of aggregates on the behaviour of concrete subjected to elevated temperature. Cement and Concrete Research 41:392-402.
73. Xing Z., Hébert R., Beaucour A.L., Ledésert B., Noumowe A. (2014). Influence of chemical and mineralogical composition of concrete aggregates on their behaviour at elevated temperature. Materials and Structures 47:1921-1940.
74. Medina C., Frías M., Sánchez de Rojas M.I. (2012) Microstructure and properties of recycled concretes using ceramic sanitary ware industry waste as coarse aggregate. Construction and Building Materials 31: 112-118.
75. Sancak E., Dursun Sari Y., Simsek O. (2008) Effects of elevated temperature on compressive strength and weight loss of the light-weight concrete with silica fume and superplasticizer. Cement and Concrete Composite 30:715-721.
76. Savva A., Manita P., Sideris K.K. (2005) Influence of elevated temperatures on the mechanical properties of blended cement concretes prepared with limestone and siliceous aggregates. Cement and Concrete Composite 27:239-248.

Please cite this document as: Meloni P., Mistretta F., Stochino F., Carcangiu G. Thermal Path Reconstruction for Reinforced Concrete Under Fire, Fire Technology, 55, 1451-1475, (2019)

77. Menéndez E., Vega L., Andrade C. (2012). Use of decomposition of portlandite in concrete fire as indicator of temperature progression into the material. Journal of Thermal Analysis and Calorimetry 110: 203-209.
78. Liu C., Wang D., Zheng H., Liu T. (2017). A dehydroxylation kinetics study of brucite Mg(OH)2 at elevated pressure and temperature. Physics and Chemistry of Minerals 44: 297-306.
79. Nazri F.M., Shahidan S., Baharuddin N.K., Beddun S., Hisyam Abu Bakar B.H. (2017). Effects of heating durations on normal concrete residual properties: compressive strength and mass loss. IOP Conference Series: Materials Science and Engineering, 271 1.
80. Toumi B., Resheidat M., Guemmadi Z., Chabil H. (2009) Coupled Effect of High Temperature and Heating Time on the Residual Strength of Normal and High-Strength Concretes. Jordan Journal of Civil Engineering 3, 322-330.
81. Zhou Q. and Glasser F.P. (2001). Thermal stability and decomposition mechanisms of ettringite at $< 120^{\circ}$C. Cement and Concrete Research 31:1333-1339.
82. De Jong, M.J., Ulm, F.J. (2007).The nanogranular behavior C-S-H at elevated temperatures (up to 700C). Cement and Concrete Research 37:1-12.
83. Török Á., Hajpál M. (2005). Effect of Temperature Changes on the Mineralogy and Physical Proper- ties of Sandstones. A Laboratory Study. Restauration Building Monuments, 4: 1-8.
84. Stepkowska E.T. (2005). Hypothetical transformation of Ca(OH)2 into CaCO3 in solid-state reactions of portland cement. Journal of Thermal Analysis and Calorimetry, 80: 727-733.

Please cite this document as: Meloni P., Mistretta F., Stochino F., Carcangiu G. Thermal Path Reconstruction for Reinforced Concrete Under Fire, Fire Technology, 55, 1451-1475, (2019)